

The Fermi Gamma-ray Burst Monitor: Results from the first two years

Andreas von Kienlin¹ on behalf of the Fermi/GBM Collaboration

Max-Planck-Institut für extraterrestrische Physik

Giessenbachstraße, 85748 Garching, Germany

E-mail: azk@mpe.mpg.de

In the first two years since the launch of the Fermi Observatory, the Gamma-ray Burst Monitor (GBM) has detected over 500 Gamma-Ray Bursts (GRBs), of which 18 were confidently detected by the Large Area Telescope (LAT) above 100 MeV. Thanks to the thick Bismuth Germanate (BGO) scintillation detectors and the high time resolution, the GBM system has unprecedented capabilities for the detection of short & hard GRBs.

Besides GRBs, GBM has triggered on other transient sources, such as Soft Gamma Repeaters (SGRs), Terrestrial Gamma-ray Flashes (TGFs) and solar flares. Here we present the science highlights of the GBM observations.

*8th INTEGRAL Workshop “The Restless Gamma-ray Universe”
Dublin, Ireland
September 27-30, 2010*

¹ Speaker

1. Introduction

The *Fermi* Gamma-ray Space Telescope (*FGST*, formerly known as *GLAST*), is an international and multi-agency space observatory, which was successfully launched on June 11, 2008. The payload comprises two science instruments, the Large Area Telescope [1], a pair conversion telescope operating in the energy range between 20 MeV and 300 GeV and the Gamma-Ray Burst Monitor (GBM) [2], which extends the *Fermi* energy range to lower energies (from 8 keV to 40 MeV); the combination of both instruments covers more than seven decades in energy. Since *Fermi* was launched into a nearly circular orbit with an altitude of 565 km and an inclination of 25.6 degrees, it allows GBM to observe the whole unocculted sky of about 9 sr at any time.

The primary role of the GBM is to augment the science return from *Fermi* in the study of GRBs by discovering transient events within a larger field of view (FoV) and performing time-resolved spectroscopy of the measured burst emission.

2. GBM Instrument and Detectors

The GBM experiment (Fig. 1) comprises two different types of scintillation detectors, a Data Processing Unit (DPU), and a Power-Supply Box. Burst locations and the low energy part of GRB spectra in the energy range from 8 keV to 1 MeV are provided by an array of 12 Thallium-activated sodium iodide (NaI) scintillator detectors. The disk-like shape of the cylindrical NaI crystals with a diameter of 12.7 cm and a thickness of 1.27 cm results in a quasi-cosine detector response with respect to the detector normal axis.

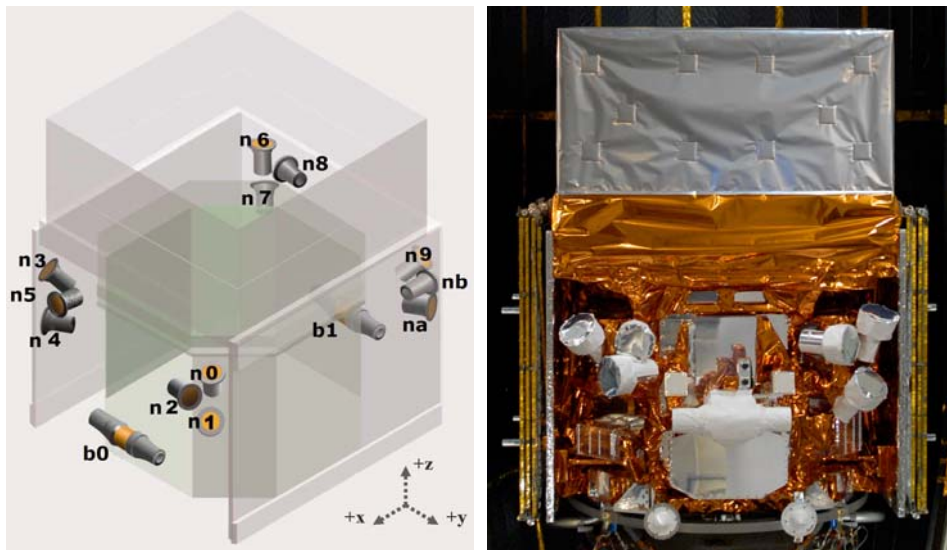


Figure 1: The Fermi Gamma-Ray Space Telescope. The left panel shows a schematics of the spacecraft with the 14 GBM detectors. The right panel shows the LAT with its reflective covering. Six of the GBM NaI detectors and one BGO detector can be seen on the side of the spacecraft. Photo credit: NASA

The NaI detectors are distributed around the outer parts of the spacecraft so that, when the radiation of a GRB arrives, the GBM can roughly determine its location from the differences between the event rates measured by the differently-inclined individual detectors. The burst locations determined by the onboard flight software are transmitted to the LAT and to the ground in near real time. Such burst alarms are forwarded as quickly as possible to interested scientists worldwide for follow-up observations.

With their energy range extending between ~ 0.2 and 40 MeV, the two Bismuth Germanate scintillation detectors (BGO) provide the overlap in energy with the LAT instrument and are crucial for the in-flight inter-instrument calibration [3]. The two cylindrical BGO crystals have a diameter and a length of 12.7 cm and are mounted on opposite sides of the Fermi spacecraft. The large effective area of a BGO detector of ~ 160 cm² over most of the energy range provides exceptional capabilities for the detection of short & hard GRBs and Terrestrial Gamma Flashes (TGFs).

A burst trigger occurs when the flight software detects an increase in the count rates of two or more detectors above an adjustable threshold specified in units of the standard deviation of the background rate. 28 different trigger algorithms operate simultaneously, each with a distinct threshold. The trigger algorithms currently implemented include four energy ranges: 50 – 300 keV, which is the standard GRB trigger range, 25 – 50 keV to increase sensitivity for Soft Gamma Repeaters (SGRs) and GRBs with soft spectra, > 100 keV, and > 300 keV to increase sensitivity for hard GRBs and Terrestrial Gamma-Ray Flashes (TGFs).

The Fermi Observatory incorporates the capability to autonomously alter the observing plan to slew to and maintain pointing at a GRB for a set period of time, nominally 5 hr, subject to earth limb constraints. This allows the LAT to observe delayed high-energy emission. Either the GBM or the LAT can generate an Autonomous Repoint Request (ARR) to point at a GRB.

3. Results from the first two years

3.1 GRB Observations

During its two years of operations since trigger enabling (July 13th, 2009 – September 6th, 2010), GBM detected ~ 540 GRBs, with ~ 270 bursts placed inside the LAT FoV [4]. For most of the 18 GRBs detected with the main instrument LAT (> 100 MeV) the GBM served as a trigger, only in the case of GRB 090510 the LAT triggered independently. The most energetic events include GRB 080916C [5], GRB 090510 [6], GRB 090902B [7], and GRB 090926A [8]. In all these cases, the LAT detected photons with energies > 10 GeV, with GRB 090902B being the record holder with 33 GeV, the highest photon energy reported so far for a GRB. In 45 cases, an ARR was positively issued by GBM to repoint the LAT and follow particularly bright events. This allowed the detection of long-lasting high-energy emission for several LAT GRBs. From the spectral point-of-view, joint GBM-LAT observations uncovered the presence of two spectral components in GRB 090902B. For this burst, a power law component dominates the Band component at both low (< 50 keV) and high (> 100 MeV) energies and is significant within just the GBM data.

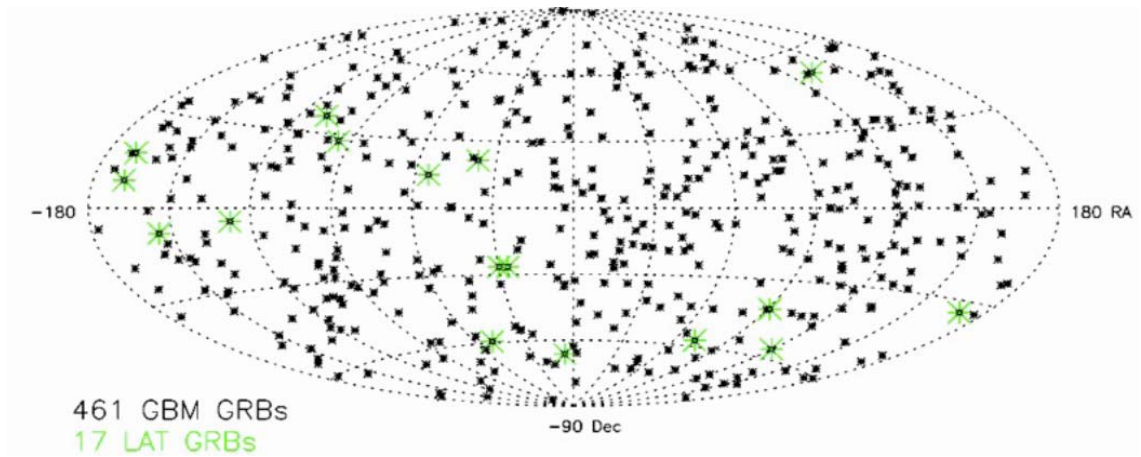


Figure 2: Fermi/GBM sky map. The 461 GRBs detected by GBM up to May 22, 2010 are shown as black crosses. The 17 GBM GRBs also observed by LAT are shown as green stars.

The overlapping FoVs of GBM and of the Burst Alert Telescope (BAT) onboard Swift [9] contribute to ~ 40 common detections/yr. The finer LAT localizations errors ($< 0.4^\circ$) resulted in Swift follow-up of several Fermi bursts, providing 8 redshifts measurements (by ground-based observatories) so far. Furthermore concurrent observations with the GBM instrument are a source of E_{Peak} for Swift bursts. GBM is extending the Swift energy range (15 - 150 keV) to higher and lower energies (8 keV - 40 MeV).

Here we present GRB observations [10] which are showing the exceptional capabilities of the GBM instrument. Especially bright (Fluence $> 2 \times 10^{-6}$ erg cm^{-2}) and short ($t_{50} < 1$ s) GRBs like GRB090227B, GRB 090228 and GRB 090510 with an exceptional hard spectrum are perfect benchmarks for the GBM instrument. The complex, multi-peaked time history of GRB090227B, shown in Fig. 3 mimics a long GRB compressed in time. As shown it is possible to perform time-resolved spectroscopy with a fine-time resolution of 2 ms. The E_{Peak} values derived from fits with the Band function [11] are compared to long GRBs, shifted towards higher energies of several MeV. The time-resolved spectral analysis exhibits a soft-to-hard and hard-to-soft variation at this fine time resolution and E_{Peak} globally tracks the lightcurve structures like in long GRBs. The time-integrated spectra of the events deviate from the Band function, indicating the existence of an additional spectral component. The time-integrated E_{Peak} values exceed 2 MeV for two of the bursts, and are well above the values observed in the brightest long GRBs. Their E_{Peak} values and their low-energy power-law indices confirm that short GRBs are harder than long ones.

3.2 GBM Catalogs

Catalogs covering the first two years of GBM GRBs are currently being produced. The main catalog [12] summarizes basic parameters for all triggered GRBs, including sky location, fluence in two energy ranges (50-300 keV and 10-1000 keV), peak flux for the same two energy ranges and three timescales (64 ms, 256 ms and 1024 ms) and duration (T_{50} and T_{90} in the 50-300 keV range). The spectroscopy catalog [13] includes spectral fits using several standard functions for all sufficiently bright GRBs. The standard functions include power-law, power-

law with exponential cut-off, Band function, and smoothly-broken power-law. For each burst two sets of spectral fits are performed: a 3.5σ signal-to-background selection for the duration of the burst (fluence spectra), and a peak count rate selection (peak flux spectra). The peak count rate interval is 1 s for long bursts and 64 ms for short bursts, based on the burst T_{90} duration.

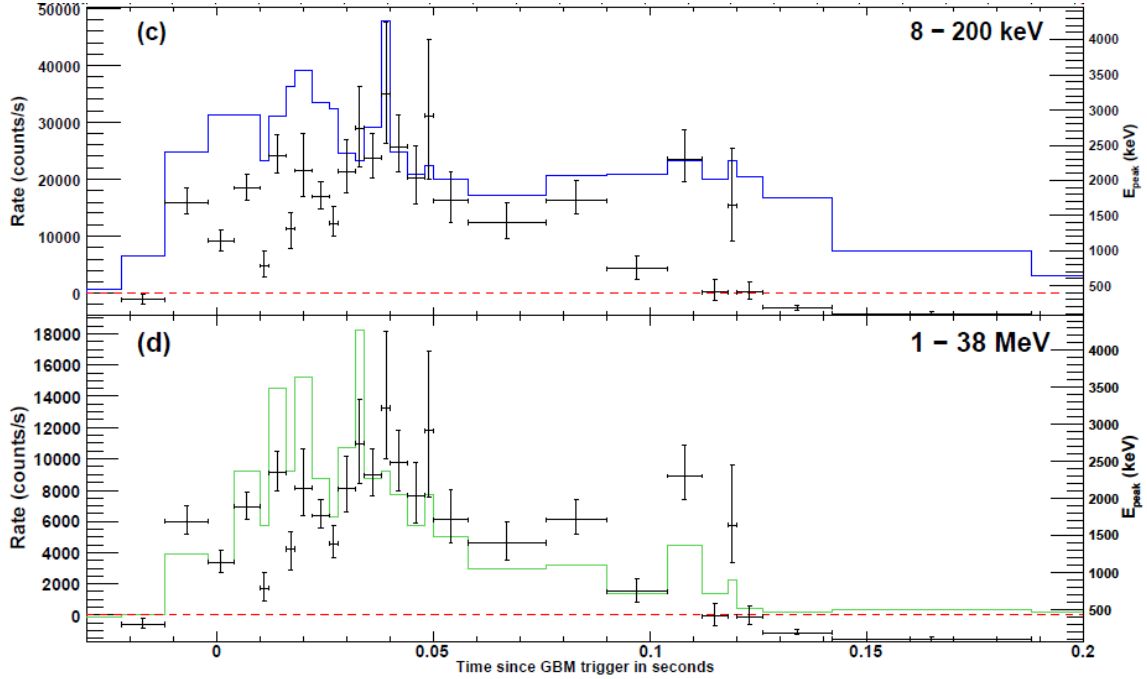


Figure 3: Multi-peaked time history of the short GRB 090227B in two energy bands (panel (c): 8 keV to 200 keV, NaI detectors) and (panel (d): 1MeV to 38 MeV, BGO detectors) with variable time bins (histograms), optimized for time resolved spectroscopy. The Band function peak energy, E_{Peak} , is plotted over the light curve for each time interval. The count rates are background subtracted.

3.3 Results on non-GRB-Observations

Apart from GRBs, GBM triggered 170 times on SGR outbursts, mostly on soft, short trigger algorithms. Those triggers originated from four different active SGRs. Of those four, one is an already known source (SGR J1806-20), two are new sources discovered with Swift (SGRJ 0501+4516 and SGR J1550-5418) and one was discovered with GBM (SGR J0418+5729) [14]. GBM also triggered 93 times from TGF signals, all on hard, short trigger algorithms. First observations of a smaller sample of TGFs and their properties are reported in [15]. The temporal properties of a considerably larger sample of TGFs observed with GBM can be found in [16], who discuss several distinct categories of TGFs mainly identified by their time profiles. Moreover, [17] recently presented a search for correlations between TGFs detected by GBM and lightning strokes measured using the World Wide Lightning Location Network (WWLLN). In addition to gamma-ray TGFs, GBM has observed several TGFs by the propagation of charged particles along geomagnetic field lines. Strong 511 keV annihilation lines have been observed, demonstrating that both electrons and positrons are present in the particle beams [18].

Finally, GBM triggered 33 times on solar flares. Several other triggers were caused by well known gamma-ray emitters, such as Cyg X-1, or by accidental particle events.

Besides triggered transient sources, which are detected by the on-board trigger algorithm, GBM can be used to study hard X-ray pulsars with periods greater than a few seconds. These are monitored using Fourier transforms and epoch folding [19]. Moreover, GBM background data is extremely useful for a number of other studies, enabling a wide range of guest investigations. These data are currently used to monitor variable X-ray sources using the earth occultation technique [20].

Acknowledgements

The Fermi GBM collaboration acknowledges support for GBM development, operations and data analysis from NASA in the US and BMWi/DLR in Germany.

References

- [1] Atwood W. B. et al., *ApJ*, 697 (2009) 1071
- [2] Meegan C. A. et al., *ApJ*, 702 (2009) 791
- [3] Bissaldi E. et al., *Exp. Astr.*, 24 (2009) 47
- [4] Bissaldi E. et al., *Nuovo Cimento C* in press (2011)
- [5] Abdo A. A. et al., *Science*, 323 (2009a) 1688
- [6] Abdo A. A. et al., *Nature*, 462 (2009b) 331
- [7] Abdo A. A. et al., *ApJ*, 707 (2009c) 580
- [8] Abdo A. A. et al., *ApJ*, submitted, arXiv:1101.2082 (2011)
- [9] Gehrels N. et al., *ApJ*, 611 (2004) 1005
- [10] Guiriec S. et al., *ApJ*, 725 (2010) 225
- [11] Band, D. et al., *ApJ*, 413 (1993) 281
- [12] Paciesas W. S. et al., *ApJ in preparation*, (2011)
- [13] Goldstein A. et al., *ApJ in preparation*, (2011)
- [14] Van der Horst A. et al., *ApJL*, 711 (2010) L1
- [15] Briggs M. S. et al., *JGR*, 115 (2010) A07323
- [16] Fishman G. J. et al., *JGR submitted*, (2011)
- [17] Connaughton V. et al., *JGR*, 115 (2010) A12307
- [18] Briggs M. S. et al., *GeoRL*, 38 (2011) L02808
- [19] Finger M. H. et al., *Fermi Symposium, eConf Proc.* (2010)
- [20] Wilson-Hodge C. A. et al., *Fermi Symposium, eConf Proc.* (2010)